

## ENVIRONMENTAL EFFECTS ON GASEOUS DISKS OF THE VIRGO SPIRAL GALAXIES<sup>1</sup>

HIROYUKI NAKANISHI,<sup>2,3</sup> NARIO KUNO,<sup>3,4</sup> YOSHIAKI SOFUE,<sup>2</sup> NAOKO SATO,<sup>5,6</sup> NAOMASA NAKAI,<sup>7</sup> YASUHIRO SHIOYA,<sup>8,9</sup>  
TOMOKA TOSAKI,<sup>3,10</sup> SACHIKO ONODERA,<sup>2</sup> KAZUO SORAI,<sup>5</sup> FUMI EGUSA,<sup>2</sup> AND AKIHIKO HIROTA<sup>3,11</sup>

Received 2004 August 29; accepted 2006 July 24

### ABSTRACT

We found high molecular fractions ( $f_{\text{mol}}$ ; ratio of the molecular to total gas surface densities) in three of five Virgo spiral galaxies in spite of their low total gas column density, based on  $^{12}\text{CO } J = 1-0$  observations with the Nobeyama 45 m telescope equipped with a multibeam receiver, BEARS. We interpret this as a result of environmental effects. Combining the CO data with H I data, the relationship between the surface density of the total gas (H I plus H<sub>2</sub>) and  $f_{\text{mol}}$  indicates that the three galaxies near the cluster center have larger  $f_{\text{mol}}$  values than expected for field galaxies, while the others show normal  $f_{\text{mol}}$ . The large  $f_{\text{mol}}$  is interpreted as being due either to effective H I gas stripping, even in the inner disks, or to large ISM pressure induced by the high ICM pressure and/or ram pressure, although the possibility of an unusually high metallicity cannot be ruled out.

*Subject headings:* galaxies: clusters: individual (Virgo) — galaxies: ISM — ISM: molecules — radio lines: ISM

### 1. INTRODUCTION

Galaxy members in a cluster of galaxies are embedded in a hot diffuse intracluster medium (ICM) emitting X-rays and suffering various environmental effects. Since Virgo is one of the nearest clusters, we can study the environmental effects there in greatest detail.

Observation in the 21 cm line show that the H I gas is deficient for galaxies near the center of the Virgo Cluster (e.g., Cayatte et al. 1990). This is interpreted as being a result of ram pressure stripping. Vollmer et al. (2001) simulated the ram pressure effect by a numerical calculation and matched well the observed distortion of the H I disk due to the ram pressure. Kenney & Young (1988, 1989) observed the Virgo spiral galaxies in the CO  $J = 1-0$  line using the 14 m telescope of the Five College Radio Astronomy Observatory (FCRAO) and found that the molecular gas content appears to be normal, even in H I-deficient galaxies. They reported that H I-deficient galaxies have a high ratio of CO flux to H I flux.

Whether a galaxy suffers environmental effects or not, the inner disk of a spiral galaxy is dominated by molecular gas, be-

cause in general the inner disk is originally dominated by molecular gas. Therefore, it has not been clarified whether the inner disk is affected by environmental effects or not.

We can enumerate three possibilities for the physical condition of the inner disk: (1) ram pressure stripping occurs only in the outer H I disk, and the inner disk suffers no environmental effect; (2) ram pressure stripping occurs in the inner disk as well as the outer disk, but only H I gas is selectively stripped; (3) the ISM pressure of the inner disk increases due to external pressures, and molecular gas formation is enhanced. The molecular gas can be dominant in the inner disk in any of these three possibilities.

In order to develop our understanding of the physical condition of the gas in inner disks of cluster spiral galaxies, we must pay attention to the molecular fraction ( $f_{\text{mol}}$ ; ratio of molecular to total gas surface density). In the first possibility, there would be no difference in the molecular fraction  $f_{\text{mol}}$  in the inner disk between cluster and field galaxies. However, the  $f_{\text{mol}}$  of cluster galaxies would be larger than that of field galaxies in the second and third possibilities.

In this paper, we show results of the highest resolution single-dish observations in the CO line of five Virgo Cluster galaxies achieved with the Nobeyama 45 m telescope equipped with a multibeam receiver, BEARS. We also compare the CO data with H I data with almost the same resolution obtained with the Very Large Array (VLA) C and D configurations. These data sets enable us to investigate the molecular fraction at each point of the spiral galaxies with a fine scale, while earlier research has dealt with the total amounts of H I and CO (H<sub>2</sub>) gases in galaxies. Based on clues from  $f_{\text{mol}}$ , we quantitatively discuss the physical condition of the gas disks in terms of (1) H I stripping, (2) external pressure due to the ICM or ram pressure, (3) intrinsic metallicity in a galaxy, and (4) the UV field of a galaxy. The distance of the Virgo Cluster is taken to be 16.1 Mpc (Ferrarese et al. 1996).

### 2. OBSERVATIONS AND DATA

The  $^{12}\text{CO } J = 1-0$  observations of the Virgo Cluster spirals were made from 2002 December to 2004 April with the Nobeyama 45 m radio telescope. The half-power beamwidth was 15'' (1.2 kpc at the Virgo Cluster) at 115 GHz. We used a focal plane array receiver, BEARS (SIS 25-BEam Array Receiver

<sup>1</sup> Part of this work was carried out under the common use observation program at the Nobeyama Radio Observatory (NRO). NRO is a branch of the National Astronomical Observatory.

<sup>2</sup> Institute of Astronomy, University of Tokyo, 2-21-1 Osawa, Mitaka, Tokyo 181-0015, Japan.

<sup>3</sup> Nobeyama Radio Observatory, Minamimaki, Minamisaku, Nagano 384-1305, Japan; hnakanis@nro.nao.ac.jp.

<sup>4</sup> Graduate University for Advanced Studies (SOKENDAI), 2-21-1 Osawa, Mitaka, Tokyo 181-0015, Japan.

<sup>5</sup> Division of Physics, Graduate School of Science, Hokkaido University, Sapporo 060-0810, Japan.

<sup>6</sup> Center for Education and Research of Lifelong Learning, Wakayama University, Wakayama 640-8510, Japan.

<sup>7</sup> Institute of Physics, University of Tsukuba, Ten-nodai, 1-1-1 Tsukuba, Ibaraki 305-8577, Japan.

<sup>8</sup> Astronomical Institute, Graduate School of Science, Tohoku University, Aramaki, Aoba, Sendai 980-8578, Japan.

<sup>9</sup> Department of Physics, Faculty of Science, Ehime University, Matsuyama 790-8577, Japan.

<sup>10</sup> Gunma Astronomical Observatory, 6860-86 Nakayama, Takayama, Agatsuma, Gunma 377-0702, Japan.

<sup>11</sup> Department of Astronomy, School of Science, University of Tokyo, Bunkyo-ku, Tokyo 113-0033, Japan.

TABLE 1  
OBSERVATIONAL PARAMETERS

NGC (1)	R.A. (J2000.0) (2)	Decl. (J2000.0) (3)	Morphology (4)	$B_T$ (mag) (5)	$i$ (deg) (6)	P.A. (deg) (7)	$V_{\text{hel}}$ (km s <sup>-1</sup> ) (8)
4254.....	12 18 49.61	+14 24 59.6	SA(s)c	10.44	42	68	2405
4402.....	12 26 07.45	+13 06 44.7	Sb	12.55	75	90	234
4569.....	12 36 49.82	+13 09 45.8	SAB(rs)ab	10.26	64	23	-235
4579.....	12 37 43.53	+11 49 05.5	SAB(rs)b	10.48	38	05	1520
4654.....	12 43 56.67	+13 07 36.1	SAB(rs)cd	11.10	52	125	1039

NOTES.—Units of right ascension are hours, minutes, and seconds, and units of declination are degrees, arcminutes, and arcseconds. Col. (1): Galaxy name. Cols. (2) and (3): Central position taken from Sofue et al. (2003). Col. (4): Morphological type from RC3 (de Vaucouleurs et al. 1991). Col. (5): Total  $B$ -band magnitude taken from RC3. Cols. (6) and (7): The inclination angle and the position angle taken from Koopmann et al. (2001) or Phookun et al. (1993). Col. (8): Systemic velocity taken from Kenney & Young (1988) or RC3.

System), which consisted of 25 beams ( $5 \times 5$ ) and was operated in the double-sideband (DSB) mode (Sunada et al. 2000). The separation between the beams was  $41''$ . Twenty-five digital autocorrelators with a 500 kHz resolution ( $1.3 \text{ km s}^{-1}$  at 115 GHz) and a 512 MHz coverage ( $1332 \text{ km s}^{-1}$ ) (Sorai et al. 2000b) were used as spectrometers.

Calibration of the line intensity was made with an absorbing chopper wheel in front of the receiver, which yielded the antenna temperature  $T_A^*$  corrected for the atmospheric and antenna ohmic losses. Since the scale of the intensity varies with the beams, mainly due to the difference of the sideband ratio between the upper sideband (USB) and the lower sideband (LSB), we scaled the observed DSB intensity to the SSB (single sideband) intensity using scaling factors that were determined by comparing the CO intensities of NGC 7538 measured with BEARS and a single-beam SSB receiver, SIS100. The main-beam efficiency of the telescope was  $\eta_{\text{MB}} = 0.40$  at 115 GHz, and the intensity given in this paper is the main-beam brightness temperature, defined by  $T_{\text{MB}} \equiv T_A^*/\eta_{\text{MB}}$ .

We mapped five Virgo galaxies with a grid spacing of  $10''$ . The number of total observed points for each galaxy was 576 and the mapped area was  $3'.95 \times 3'.95$ , except for NGC 4254 and NGC 4569, whose number of observed points was 1056 and the area was  $3'.95 \times 7'.38$ . The observations were made in the position-switching mode with an off-position at an offset of  $7'$  from the centers of the galaxies in azimuth. The typical rms noise of the main-beam brightness temperature was  $\Delta T_{\text{MB}} = 0.09\text{--}0.18 \text{ K}$  per velocity channel. Pointing of the antenna was calibrated by observing the continuum point source 3C 273 at 43 GHz, and its typical error was less than  $5''$  (peak value). Our observed samples were selected out of the galaxies in Sofue et al. (2003), and the observing parameters are listed in Table 1.

To compare with the distribution of CO, we used the H I data of the target galaxies mapped with the VLA. The H I data were adopted from Phookun et al. (1993) for NGC 4254, from Cayatte et al. (1990) for NGC 4402, NGC 4569, and NGC 4579, and from Phookun & Mundy (1995) for NGC 4654. The spatial resolution of the H I maps was about  $20''$ , which is close to that of our CO maps. Table 2 summarizes the parameters of the H I data.

Figure 1 shows the distribution of the CO integrated intensity,  $I_{\text{CO}} \equiv \int T_{\text{MB}} dv$  (K km s<sup>-1</sup>) (*colors*), and the H I intensity (*contours*) of the five galaxies. The CO emissions distribute in the inner disks, and the extensions are typically up to radii of  $\sim 1.5$  (7 kpc).

The H I gas in NGC 4254 and NGC 4654 is abundant, and its distribution is strongly distorted. The H I disks of NGC 4402 and NGC 4569 are truncated at the edges of the CO disks. In NGC

4579, the H I gas surrounds the central CO disk where the H I gas is deficient.

### 3. ENVIRONMENTAL EFFECTS ON GASEOUS DISKS

#### 3.1. Molecular Fraction as a Function of the Surface Density of the Total Gas

The fraction of molecular gas to the total gas (H I gas plus H<sub>2</sub> gas),  $f_{\text{mol}}$ , is determined by the ISM (interstellar medium) pressure  $P$ , metallicity  $Z$ , and UV radiation  $U$  (Elmegreen 1993). Here the molecular fraction  $f_{\text{mol}}$  is defined as

$$f_{\text{mol}} \equiv \frac{\Sigma_{\text{H}_2}}{\Sigma_{\text{H}_1} + \Sigma_{\text{H}_2}}, \quad (1)$$

with  $\Sigma_{\text{H}_1}$  and  $\Sigma_{\text{H}_2}$  being the surface mass densities of H I and H<sub>2</sub>, respectively. Since the ISM pressure is approximately proportional to the square of the gas surface density (Elmegreen 1993),

$$\frac{P}{P_0} = \frac{\Sigma^2}{\Sigma_0^2} = \frac{(\Sigma_{\text{H}_1} + \Sigma_{\text{H}_2})^2}{(\Sigma_{\text{H}_1} + \Sigma_{\text{H}_2})_0^2}, \quad (2)$$

$f_{\text{mol}}$  is expressed as a function of  $\Sigma$ , when  $Z$  and  $U$  are given. Honma et al. (1995), Kuno et al. (1995), and Sorai et al. (2000a) investigated  $f_{\text{mol}}$  in nearby spiral galaxies, and showed that it is well reproduced by a model of Elmegreen (1993). Figure 2 shows model curves of the  $\Sigma$ - $f_{\text{mol}}$  relation calculated based on Elmegreen (1993), where we scale  $P$ ,  $U$ , and  $Z$  with the values of the solar neighborhood:  $P_0$ ,  $U_0$ , and  $Z_0$ . The gas surface density

TABLE 2  
H I DATA PARAMETER

NGC (1)	Synthesized Beam Size (arcsec <sup>2</sup> ) (2)	$\Delta V$ (km s <sup>-1</sup> ) (3)	$\Delta T_B$ (K) (4)	Reference (5)
4254.....	$25 \times 24$	10.3	0.45	1
4402.....	$21 \times 17$	25.0	1.7	2
4569.....	$17 \times 13$	25.0	2.8	2
4579.....	$19 \times 18$	25.0	2.7	2
4654.....	$24 \times 25$	10.3	0.44	3

NOTES.—Col. (1): Galaxy name. Col. (2): Synthesized beam size. Col. (3): Velocity resolution. Col. (4): rms noise in brightness temperature.

REFERENCES.—(1) Phookun et al. 1993; (2) Cayatte et al. 1990; (3) Phookun & Mundy 1995.

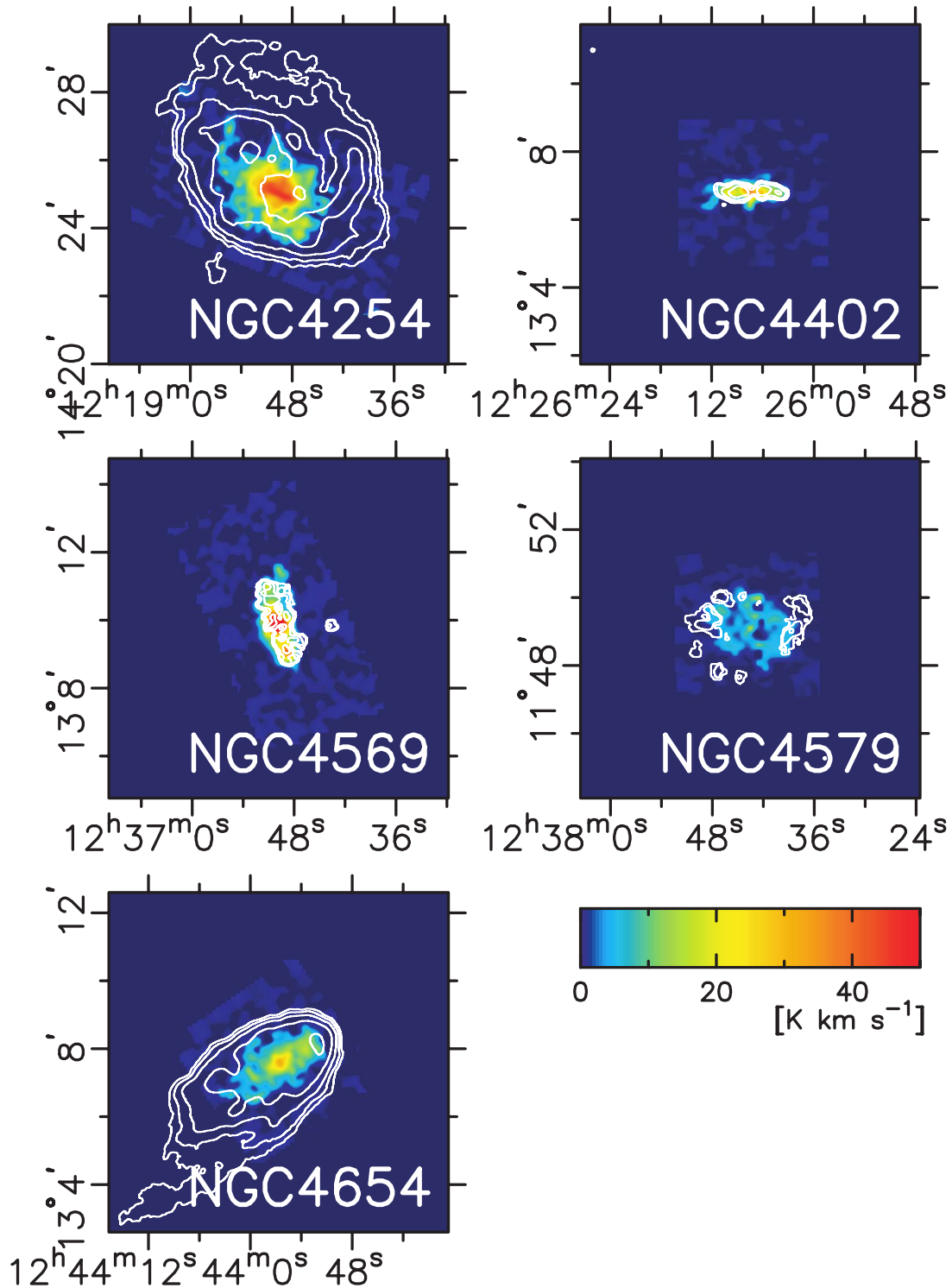


FIG. 1.—Integrated CO intensity maps (colors) and the integrated H I intensity maps (contours). The contour levels are 100, 200, 400, 800, and 1600  $\text{K km s}^{-1}$ .

at the solar neighborhood,  $\Sigma_0$ , is taken to be  $8 M_{\odot} \text{pc}^{-2}$  (Sanders et al. 1984), which is adopted to be proportional to  $P_0^{1/2}$ . We show model curves taking UV radiations of  $0.1U_0$ ,  $1U_0$ , and  $10U_0$  and metallicities of  $0.1Z_0$ ,  $1Z_0$ , and  $10Z_0$ .

Figure 3 shows  $f_{\text{mol}}$  against  $\Sigma$  for each observed point of the five galaxies, where the CO-to- $\text{H}_2$  conversion factor was adopted to be  $X_{\text{CO}} = 1.0 \times 10^{20} \text{H}_2 \text{cm}^{-2} \text{K}^{-1} \text{km}^{-1} \text{s}$  (Nakai & Kuno 1995). The dashed curves in all panels denote the averaged  $f_{\text{mol}}$  of NGC 4254 and NGC 4654. The molecular frac-

tions  $f_{\text{mol}}$  of NGC 4254 and NGC 4654 show similar curves to the models with  $U = 1U_0$  and  $Z = 1Z_0$ , which is expected for field galaxies.

On the contrary, the other three galaxies (NGC 4402, NGC 4569, and NGC 4579) present larger molecular fractions than the dashed curve. NGC 4402 shows an extraordinarily large  $f_{\text{mol}}$  in spite of the small surface density of the gas. For NGC 4569 the plotted points are scattered on the upper side of the dashed curve. NGC 4579 shows a very large  $f_{\text{mol}}$  in spite of the small surface

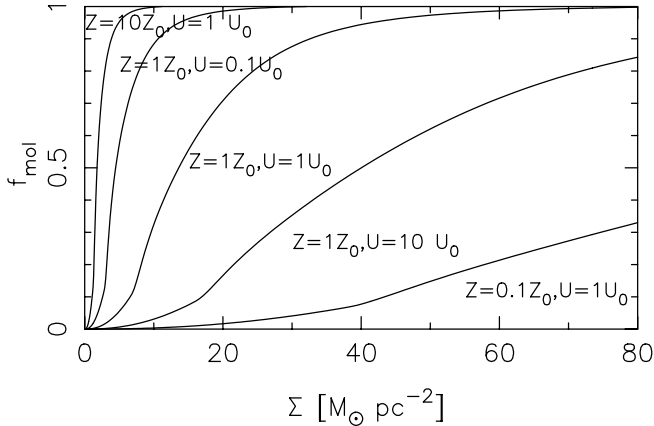


FIG. 2.—Molecular fraction  $f_{\text{mol}}$  against the surface density of the total gas  $\Sigma$  calculated using a formula of Elmegreen (1993).

density of the gas as NGC 4402. In the three galaxies,  $f_{\text{mol}}$  is always larger than the dashed curve.

### 3.2. Origin of the Unusual Molecular Fraction in the Virgo Spirals

#### 3.2.1. Ram Pressure Stripping

Ram pressure stripping is a possible interpretation of the unusually large  $f_{\text{mol}}$  of NGC 4402, NGC 4569, and NGC 4579.

Ram pressure stripping would occur if the criterion

$$\left(\frac{\rho_{\text{ICM}}}{\rho_{\text{ISM}}}\right) \left(\frac{R}{d}\right) \left(\frac{\delta v}{V_{\text{rot}}}\right)^2 > 1 \quad (3)$$

is satisfied, where  $\rho_{\text{ISM}}$  and  $\rho_{\text{ICM}}$  are the volume number density of the ISM and the ICM, respectively,  $R$  is the galactocentric radius of the element,  $d$  is the thickness of the gas disk,  $\delta v$  is the relative velocity of an ISM cloud against the ICM, and  $V_{\text{rot}}$  is the rotational velocity of the galaxy.

For a simple case, we consider a gas disk with thickness  $d \sim 0.05$  kpc, rotating at  $V_{\text{rot}} \sim 200$  km s $^{-1}$ . For a typical ICM wind with  $\rho_{\text{ICM}} \sim 10^{-4}$  H cm $^{-3}$  and  $\delta v \sim 1000$  km s $^{-1}$  (Hidaka & Sofue 2002), we obtain for the criterion of where ram pressure stripping can occur

$$\rho_{\text{ISM}} < 0.05 \left(\frac{R}{\text{kpc}}\right) \text{H cm}^{-3}. \quad (4)$$

The H I gas can be dominant in the interarm region even in inner disks, and its density typically ranges from 0.01 to 1 H cm $^{-3}$ . Hence, the H I gas can be stripped even in the inner disks. On the other hand, the molecular cloud can hardly be stripped because the gas density in the molecular cloud is 10–1000 H $_2$  cm $^{-3}$ . Therefore, the H I gas can be stripped selectively from a disk, although the molecular gas still remains in the disk. In this case,  $f_{\text{mol}}$  in the  $\Sigma$ - $f_{\text{mol}}$  diagram moves toward the upper left side of the  $\Sigma$ - $f_{\text{mol}}$  curve of field galaxies.

NGC 4402, NGC 4569, and NGC 4579 are located within the projected radius of 2 $^\circ$  from M87 at the center of the cluster, and are known to be H I deficient. Hence, they must have experienced ram pressure stripping of the H I gas. We emphasize that in these three galaxies, (1) the H I disks are restricted within the central CO disks of 1.5 radii (7 kpc) (Fig. 1), (2) the H I clouds can satisfy the

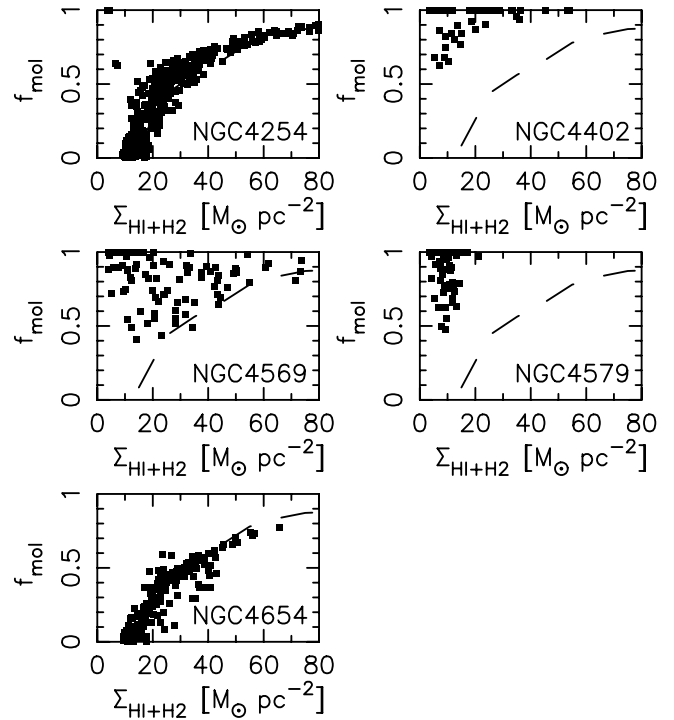


FIG. 3.—Molecular fraction  $f_{\text{mol}}$  against the surface density of the total gas  $\Sigma$ . The dashed curves in all panels denote the averaged  $f_{\text{mol}}$  of NGC 4254 and NGC 4654. The data of  $\Sigma_{\text{HI}} > 3.8 \times 10^{20}$  H cm $^{-2}$  or  $\Sigma_{\text{H}_2} > 7.0 \times 10^{19}$  H $_2$  cm $^{-2}$  ( $3\sigma$ ) are plotted.

criterion of ram pressure stripping while the molecular clouds cannot, and (3) the  $\Sigma$ - $f_{\text{mol}}$  diagrams show unusually large  $f_{\text{mol}}$ , indicating that the inner disks are highly H I deficient (Fig. 3). These three facts support the scenario that the ram pressure stripping of H I gas occurred even in the inner disks.

On the other hand, NGC 4254 and NGC 4654 are located as far as  $\sim 3^\circ$  from the center of the cluster. They show the H I distribution extending to the outer disks and the  $\Sigma$ - $f_{\text{mol}}$  relation being the same as that of field galaxies. Hence, most of the H I gas must have not yet been stripped in spite of the strongly distorted H I disks.

#### 3.2.2. Higher External Pressure due to the ICM Pressure or Ram Pressure

Another possibility for making  $f_{\text{mol}}$  large is a higher external pressure due to the ICM pressure or the ram pressure, which might make the ISM pressure larger than that estimated by the surface density.

The ICM pressure affects all gas disks isotropically. The typical density and temperature of the ICM at the Virgo Cluster are  $\rho \sim 10^{-4}$  cm $^{-3}$  and  $T \sim 10^7$  K, respectively (Nulsen & Böhringer 1995). On the other hand, the typical density and temperature of the interstellar molecular gas are  $\rho \sim 10^2$  cm $^{-3}$  and  $T \sim 10$  K, respectively. Since the pressure  $P$  is proportional to  $\rho T$ , the ICM pressure and ISM pressure are comparable to each other near the cluster center.

The ram pressure would also increase the ISM pressure if the ISM were not stripped, as mentioned by Kenney & Young (1989). The typical velocity of a galaxy is  $\sim 1000$  km s $^{-1}$  near the Virgo Cluster center. The velocity dispersion of a molecular cloud is typically  $\sim 1$  km s $^{-1}$ . Since the pressure  $P$  is proportional to  $\rho v^2$ , the ram and the ISM pressures are comparable near the cluster center.

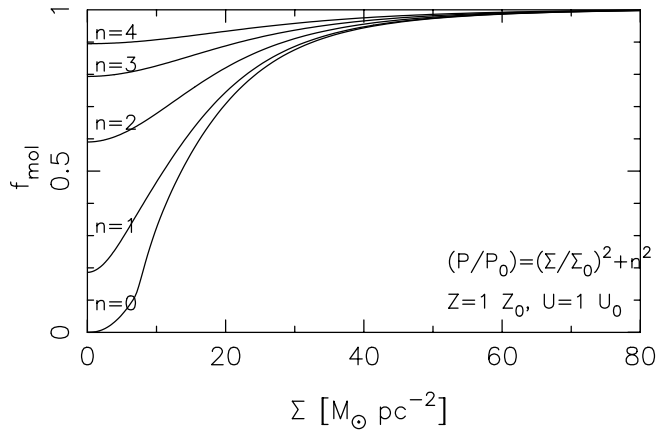


FIG. 4.—Molecular fraction  $f_{\text{mol}}$  against the surface density of the total gas  $\Sigma$  calculated using a formula of Elmegreen (1993) and adopting  $P/P_0 = (\Sigma/\Sigma_0)^2 + n^2$  ( $n = 0, 1, 2, 3,$  and  $4$ ).

As a result, the ISM pressure would increase and the higher ISM pressure would make  $f_{\text{mol}}$  larger.

We present the  $\Sigma$ - $f_{\text{mol}}$  relation in Figure 4, adopting  $P/P_0 = (\Sigma/\Sigma_0)^2 + n^2$ . The second term indicates an increment of the ISM pressure due to the ICM or the ram pressure. Figure 4 shows that the ICM pressure makes  $f_{\text{mol}}$  much larger. Thus, we can conclude that a higher external pressure due to ICM or ram pressure could be the origin of the large  $f_{\text{mol}}$ .

### 3.2.3. Larger Metallicity

Because the metallicity strongly affects  $f_{\text{mol}}$ , the larger metallicity might be an origin of the large  $f_{\text{mol}}$ . In order to examine whether the large metallicity makes  $f_{\text{mol}}$  large, data on the metallicity distributions are necessary. However, there is no available data for these galaxies, except for NGC 4254. Therefore, we below present a new idea to calculate the metallicity distribution using the CO, H I, and H $\alpha$  data instead of using the metallicity data.

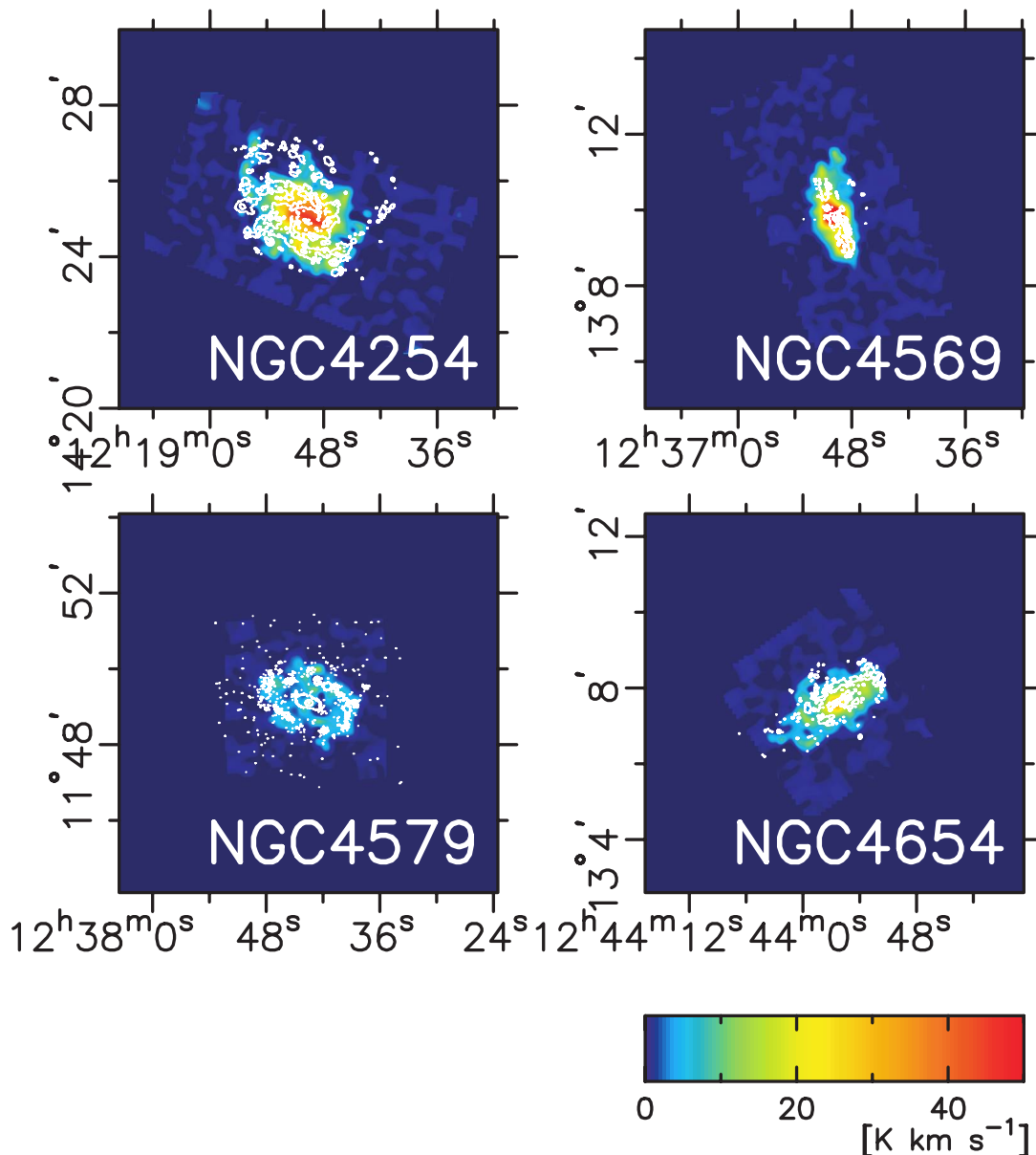


FIG. 5.—Integrated CO intensity maps (colors) and the H $\alpha$  maps (contours). The contour levels are  $2.7 \times 10^{-16}$  and  $2.7 \times 10^{-15}$  ergs  $\text{cm}^{-2}$   $\text{s}^{-1}$   $\text{arcsec}^{-2}$ .

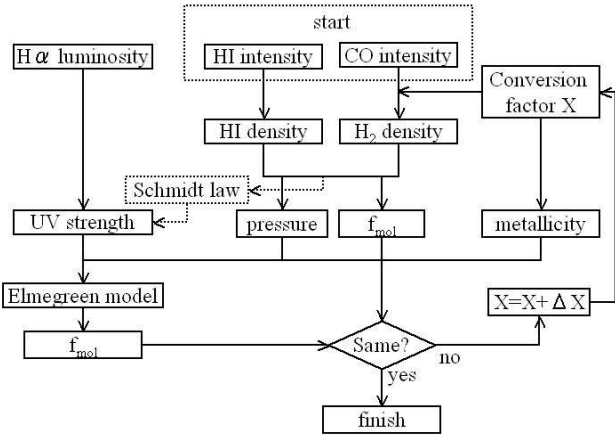


FIG. 6.—Flow chart for calculating the metallicity using H I, CO, and H $\alpha$  data.

The metallicity is expressed using the oxygen abundance  $12 + \log(O/H)$ , which is correlated with the conversion factor  $X$  (Arimoto et al. 1996). We here define

$$\log Z = 12 + \log(O/H) \quad (5)$$

and adopt the relationship

$$\log\left(\frac{X}{10^{20}}\right) = -\log Z + 9.3. \quad (6)$$

The metallicity of the solar neighborhood  $\log Z_0$  is taken to be 8.9. We can calculate the H $_2$  surface density using  $X$  if  $Z$  is given. Combining the H I and H $_2$  surface densities, we obtain the total gas density  $\Sigma$ , which gives the pressure  $P$  based on equation (2).

The UV strength can be calculated using the H $\alpha$  data. H $\alpha$  images of the Virgo Cluster galaxies, except for NGC 4402, were archived by Koopmann et al. (2001). Figure 5 shows contours of H $\alpha$  superimposed onto the CO images. We convolved the H $\alpha$  image with the same beams as the H I data. We adopted  $U_0 = 2.42 \times 10^{-7}$  ergs cm $^{-2}$  s $^{-1}$  sr $^{-1}$  (Reynolds 1984). For NGC 4402, we estimated  $U$  while considering the Schmidt law,

$$U = U_0 \left(\frac{\Sigma}{\Sigma_0}\right)^n, \quad (7)$$

where we adopted  $n = 1.33$  (Komugi et al. 2005).

Thus, we can calculate  $X$ ,  $P$ , and  $U$  if  $Z$  is given. Using obtained  $P$ ,  $U$ , and  $Z$ , we can calculate the molecular fraction  $f_{\text{mol}}$  based on the model of Elmegreen (1993). On the other hand, we can independently calculate  $f_{\text{mol}}$  using only the H I and H $_2$  surface densities. We search for an appropriate metallicity, which gives the same  $f_{\text{mol}}$  in the two ways. The searching range of the metallicity is adopted to be  $6.68 < \log Z < 11.12$ . This procedure is presented as a flowchart in Figure 6.

We plotted the calculated metallicity against the radius for each galaxy (Fig. 7). Each point corresponds to each observed point. The metallicities of NGC 4254 and NGC 4654 show that  $\log Z$  is about 9.5–10 at the galactic center, and that it gradually declines. The metallicity of NGC 4254 was calculated by Vila-Costas & Edmunds (1992) and Zaritsky et al. (1994). Our obtained values are almost consistent with their results.

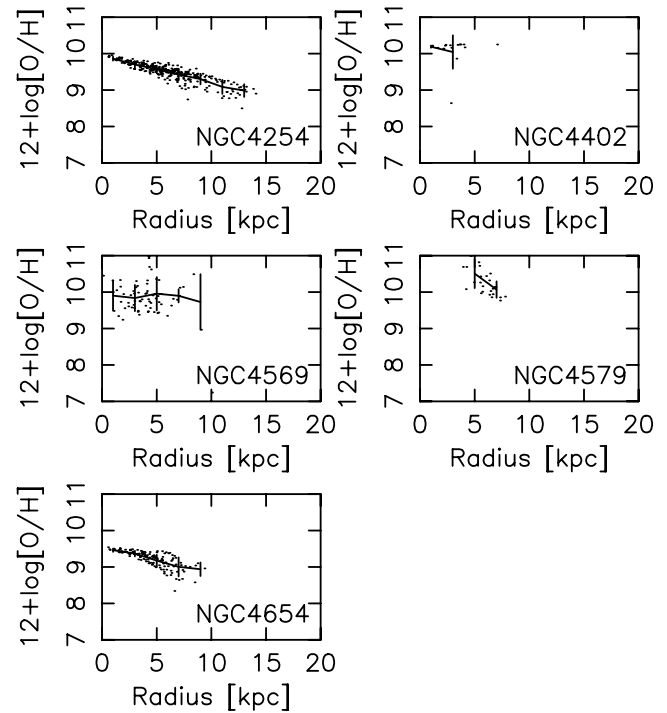


FIG. 7.—Metallicity  $\log Z = 12 + \log(O/H)$  against the radius. The metallicities were calculated using the data of  $\Sigma_{\text{HI}} > 3.8 \times 10^{20}$  H cm $^{-2}$  or  $\Sigma_{\text{H}_2} > 7.0 \times 10^{19}$  H $_2$  cm $^{-2}$  ( $3\sigma$ ). The solid curves and vertical segments indicate the mean values and standard deviations at each radius.

On the other hand, the metallicities  $\log Z$  of NGC 4402, NGC 4569, and NGC 4579 often exceed 10. However, the former research shows that there is no galaxy that gives  $\log Z > 10$ . In addition, the dispersions of  $\log Z$  of NGC 4402, NGC 4569, and NGC 4579 are larger than the others. Moreover, the metallicities  $\log Z$  of NGC 4402 and NGC 4569 increase with the radius. This tendency is unnatural because the metallicity  $\log Z$  usually decreases with the radius (Vila-Costas & Edmunds 1992; Zaritsky et al. 1994). In the case of NGC 4579, there are many points where  $Z$  cannot be calculated within the solution range  $6.68 < \log Z < 11.12$  in the inner region.

Therefore, the possibility of higher metallicity is less plausible, because an abnormal metallicity distribution is necessary to reproduce such a large  $f_{\text{mol}}$ . However, this possibility still cannot

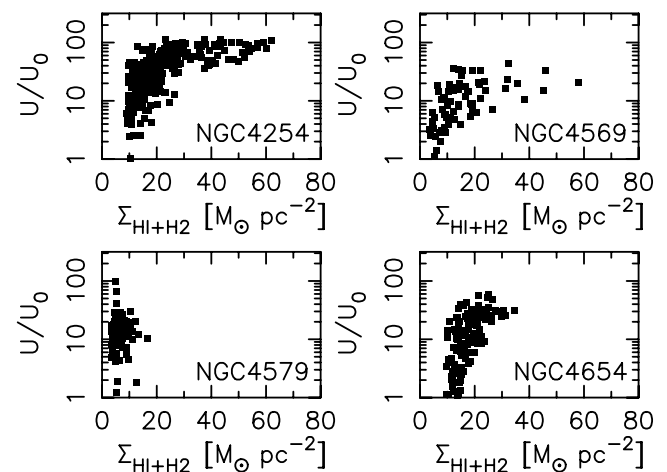


FIG. 8.—Relationship between the UV strength ( $U/U_0$ ) and surface density of the total gas  $\Sigma$ .

be ruled out, since nobody has directly measured the metallicities of NGC 4402, NGC 4569, and NGC 4579.

### 3.2.4. Lower UV Radiation Field

Because the UV strength affects  $f_{\text{mol}}$ , a lower UV radiation field might be the origin of the large  $f_{\text{mol}}$ . In order to examine this effect, we plotted the relation between the UV strength and the total gas density (Fig. 8), excluding the central 1 kpc to avoid H $\alpha$  emission from active galactic nuclei. This figure shows that there is little difference in the UV strength,  $U/U_0$ , for  $\Sigma < 20 M_{\odot} \text{pc}^{-2}$ , although  $U/U_0$  is lower in NGC 4569 than in NGC 4254 and NGC 4654 in the case of  $\Sigma > 20 M_{\odot} \text{pc}^{-2}$ . Thus, it is difficult to attribute the large  $f_{\text{mol}}$  to a lower UV radiation field, because a large  $f_{\text{mol}}$  for  $\Sigma < 20 M_{\odot} \text{pc}^{-2}$  cannot be explained by a difference in the UV strength.

## 4. SUMMARY

We observed five Virgo spiral galaxies with the NRO 45 m telescope with BEARS in the  $^{12}\text{CO} J = 1-0$  line. Comparing the CO data with the H I data to investigate the environmental effect, we found that (1) the H I gas disks of NGC 4402, NGC 4569, and NGC 4579, located near the center of the cluster, are restricted within the inner disks, (2) the H I clouds can satisfy the criterion of the ram pressure stripping, while the molecular clouds cannot, and (3) the  $\Sigma$ - $f_{\text{mol}}$  diagrams of the three galaxies show an unusually large  $f_{\text{mol}}$  for a low total gas column density. This large  $f_{\text{mol}}$  might imply that the H I gas is selectively stripped. On the other

hand, NGC 4254 and NGC 4654, located far from the cluster center, have extended H I disks and show the normal  $f_{\text{mol}}$  expected for field galaxies. Most of the H I gas of these two galaxies must not have been stripped, in spite of the strongly distorted H I disks.

A higher external pressure due to the ICM pressure and/or ram pressure might be another possibility causing the unusually large  $f_{\text{mol}}$ .

Moreover, we examined whether differences in the intrinsic conditions (metallicity and UV) cause the unusually large  $f_{\text{mol}}$ . As a result, we found that an unusually high metallicity is necessary to explain such a large  $f_{\text{mol}}$ , although it still cannot be ruled out.

We also found that the large  $f_{\text{mol}}$  cannot be explained by only a difference in the UV radiation field.

From these discussions, we note that the  $\Sigma$ - $f_{\text{mol}}$  diagram is a good tool for investigating the environmental effect. An abnormal  $f_{\text{mol}}$  indicates that the ISM suffers cluster environmental effects: ram pressure stripping or higher external pressure.

We are grateful to the members of the Nobeyama Radio Observatory. We appreciate that M. Honma kindly provided his code to calculate  $f_{\text{mol}}$ . We would also like to thank T. Namba for his help with observations and reductions. F. E. is financially supported by a research fellowship from the Japan Society for the Promotion of Science for Young Scientists.

## REFERENCES

- Arimoto, N., Sofue, Y., & Tsujimoto, T. 1996, PASJ, 48, 275  
 Cayatte, V., van Gorkom, J. H., Balkowski, C., & Kotanyi, C. 1990, AJ, 100, 604  
 de Vaucouleurs, G., de Vaucouleurs, A., Corwin, H. G., Buta, R. J., Paturel, G., & Fouqué, P. 1991, Third Reference Catalogue of Bright Galaxies (Berlin: Springer)  
 Elmegreen, B. G. 1993, ApJ, 411, 170  
 Ferrarese, L., et al. 1996, ApJ, 464, 568  
 Hidaka, M., & Sofue, Y. 2002, PASJ, 54, 33  
 Honma, M., Sofue, Y., & Arimoto, N. 1995, A&A, 304, 1  
 Kenney, J. D., & Young, J. S. 1988, ApJS, 66, 261  
 Kenney, J. D. P., & Young, J. S. 1989, ApJ, 344, 171  
 Komugi, S., Sofue, Y., Nakanishi, H., Onodera, S., & Egusa, F. 2005, PASJ, 57, 733  
 Koopmann, R. A., Kenney, J. D. P., & Young, J. 2001, ApJS, 135, 125  
 Kuno, N., Nakai, N., Handa, T., & Sofue, Y. 1995, PASJ, 47, 745  
 Nakai, N., & Kuno, N. 1995, PASJ, 47, 761  
 Nulsen, P. E. J., & Böhringer, H. 1995, MNRAS, 274, 1093  
 Phookun, B., & Mundy, L. G. 1995, ApJ, 453, 154  
 Phookun, B., Vogel, S. N., & Mundy, L. G. 1993, ApJ, 418, 113  
 Reynolds, R. J. 1984, ApJ, 282, 191  
 Sanders, D. B., Solomon, P. M., & Scoville, N. Z. 1984, ApJ, 276, 182  
 Sofue, Y., Koda, J., Nakanishi, H., Onodera, S., Kohno, K., Tomita, A., & Okumura, S. K. 2003, PASJ, 55, 1189  
 Sorai, K., Nakai, N., Kuno, N., Nishiyama, K., & Hasegawa, T. 2000a, PASJ, 52, 785  
 Sorai, K., Sunada, K., Okumura, S. K., Iwasa, T., Tanaka, A., Natori, K., & Onuki, H. 2000b, Proc. SPIE, 4015, 86  
 Sunada, K., Yamaguchi, C., Nakai, N., Sorai, K., Okumura, S. K., & Ukita, N. 2000, Proc. SPIE, 4015, 237  
 Vila-Costas, M. B., & Edmunds, M. G. 1992, MNRAS, 259, 121  
 Vollmer, B., Cayatte, V., Balkowski, C., & Duschl, W. J. 2001, ApJ, 561, 708  
 Zaritsky, D., Kennicutt, R. C., & Huchra, J. P. 1994, ApJ, 420, 87